

Interpolatory model reduction of dynamical systems with root mean squared error

Sean Reiter* Steffen W. R. Werner†

**Department of Mathematics, Virginia Tech, Blacksburg, VA 24061, USA.*

Email: seanr7@vt.edu, ORCID: [0000-0002-7510-1530](https://orcid.org/0000-0002-7510-1530)

†Department of Mathematics and Division of Computational Modeling and Data Analytics, Academy of Data Science, Virginia Tech, Blacksburg, VA 24061, USA.

Email: steffen.werner@vt.edu, ORCID: [0000-0003-1667-4862](https://orcid.org/0000-0003-1667-4862)

Abstract: The root mean squared error is an important measure used in a variety of applications such as structural dynamics and acoustics to model averaged deviations from standard behavior. For large-scale systems, simulations of this quantity quickly become computationally prohibitive. Classical model order reduction techniques attempt to resolve this issue via the construction of surrogate models that emulate the root mean squared error measure using an intermediate linear system. However, this approach requires a potentially large number of linear outputs, which can be disadvantageous in the design of reduced-order models. In this work, we consider directly the root mean squared error as the quantity of interest using the concept of quadratic-output models and propose several new model reduction techniques for the construction of appropriate surrogates. We test the proposed methods on a model for the vibrational response of a plate with tuned vibration absorbers.

1 Introduction

The modeling and numerical simulation of large-scale dynamical systems are powerful tools for deciphering the behaviour of complex physical phenomena. Such large-scale systems typically arise from the demand for highly accurate predictions. The systems that we consider in this work are described in the frequency (Laplace) domain by linear frequency-dependent algebraic equations of the form

$$(s\mathbf{E} - \mathbf{A})\mathbf{x}(s) = \mathbf{b}u(s), \quad (1)$$

where $\mathbf{E}, \mathbf{A} \in \mathbb{C}^{n \times n}$ and $\mathbf{b} \in \mathbb{C}^n$. The internal state is given by $\mathbf{x}: \mathbb{C} \rightarrow \mathbb{C}^n$, and $u: \mathbb{C} \rightarrow \mathbb{C}$ is the external input. For simplicity, we assume throughout this paper that \mathbf{E} is a nonsingular matrix. Systems of equations of the form (1) are used to model a wide range of different dynamical behaviors including heat transfers, fluid dynamics or the deformation of mechanical structures; see, for example, [6, 22].

In regards of applications, typically not the full state of (1) is observed but only a limited number of quantities of interest. In this work, we consider the case that the *root mean squared (RMS) error* of the state \mathbf{x} in (1) is measured

with respect to a point of reference $\tilde{\mathbf{x}} \in \mathbb{C}^n$. That is, we are interested in the observable $y: \mathbb{C} \rightarrow \mathbb{C}$ defined as

$$y(s) = \sqrt{\sum_{k=1}^n |q_k|^2 |x_k(s) - \tilde{x}_k|^2}, \quad (2)$$

where $x_k(s)$ is the k -th component of the state vector $\mathbf{x}(s)$, \tilde{x}_k is the k -th component of the reference point $\tilde{\mathbf{x}}$, and the scalars $q_k \in \mathbb{C}$ are weights. Systems that consider (2) as the observable quantity of interest arise in a variety of different applications, for example, in the study of structural dynamics and vibro-acoustic systems [4, 21], wherein one might be interested in the average spatial deformation or displacement of a given surface. Other examples for the use of (2) include observables relating to a system's internal energy [15], the variance of a random variable in stochastic models [16], and approximations of the cost function in quadratic regulator problems [8]. For the simplicity of presentation, we assume without loss of generality the reference state to be the zero state, $\tilde{\mathbf{x}} = \mathbf{0}_n$. This is always possible by appropriately substituting the state \mathbf{x} in (1).

Classically, the RMS error (2) of the dynamical system (1)

is simulated implicitly by introducing a linear output operator $\mathbf{C} \in \mathbb{C}^{p \times n}$ and working with a linear input-output system of the form

$$\Sigma_{\text{LO}}: \begin{cases} (s\mathbf{E} - \mathbf{A})\mathbf{x}(s) = \mathbf{b}u(s), \\ \mathbf{z}(s) = \mathbf{C}\mathbf{x}(s), \end{cases} \quad (3)$$

with the vector-valued output signal $\mathbf{z}: \mathbb{C} \rightarrow \mathbb{C}^p$. The RMS error (2) can easily be recovered from (3) by choosing

$$\mathbf{C} = [q_{i_1}\mathbf{e}_{i_1} \quad q_{i_2}\mathbf{e}_{i_2} \quad \dots \quad q_{i_p}\mathbf{e}_{i_p}]^\top,$$

where $\mathbf{e}_{i_j} \in \mathbb{C}^n$ is the i_j -th canonical basis vector and $i_1, i_2, \dots, i_p \subseteq \{1, \dots, n\}$ are the indices corresponding to the nonzero weights q_j in (2). Then, for any $s \in \mathbb{C}$, the RMS error $y(s)$ in (2) is given via the ℓ_2 -norm of the output of (3):

$$\|\mathbf{z}(s)\|_2 = \sqrt{(\mathbf{C}\mathbf{x}(s))^\mathbf{H}(\mathbf{C}\mathbf{x}(s))} = y(s),$$

where $\mathbf{w}^\mathbf{H}$ denotes the conjugate transpose of a vector $\mathbf{w} \in \mathbb{C}^n$. The frequency domain input-to-output map of the linear system (3) is fully characterized by the corresponding transfer function $\mathbf{G}: \mathbb{C} \rightarrow \mathbb{C}^p$ such that $\mathbf{z}(s) = \mathbf{G}(s)u(s)$, where

$$\mathbf{G}(s) = \mathbf{C}(s\mathbf{E} - \mathbf{A})^{-1}\mathbf{b}. \quad (4)$$

A drawback of using (3) comes in the form of a potentially large number of outputs p . This stands in contrast to the one-dimensional quantity of interest (2) and is typically disadvantageous in the design of reduced-order models.

We consider here a different approach to combine (1) with (2). By introducing a single quadratic-output function, the RMS error can be directly simulated up to the square root. Such systems with quadratic output can be written as

$$\Sigma_{\text{QO}}: \begin{cases} (s\mathbf{E} - \mathbf{A})\mathbf{x}(s) = \mathbf{b}u(s), \\ y(s)^2 = \mathbf{x}(s)^\mathbf{H}\mathbf{Q}\mathbf{x}(s), \end{cases} \quad (5)$$

where $\mathbf{Q} \in \mathbb{R}^{n \times n}$ is Hermitian. Colloquially, we refer to systems of the form (5) as *linear quadratic-output systems*. The RMS error of \mathbf{x} is easily retrieved by defining the output matrix \mathbf{Q} in (5) as the diagonal matrix with the weights $|q_k|^2 \geq 0$ as entries, i.e.,

$$\mathbf{Q} = \text{diag}(|q_1|^2, |q_2|^2, \dots, |q_n|^2).$$

In practical applications, the state dimension of (5) becomes easily very large ($n \in \mathcal{O}(10^5)$ or larger) due to the demand for highly accurate models. In this case, any repeated action involving the full-order model (5) commands significant computational resources such as time and memory.

A remedy to this problem is *model order reduction*, which is concerned with the construction of low-order, cheap-to-evaluate surrogate systems that can be used in place of the full-order model. In this work, we consider the construction of reduced-order models for linear quadratic-output systems of the form (5) given as

$$\hat{\Sigma}_{\text{QO}}: \begin{cases} (s\hat{\mathbf{E}} - \hat{\mathbf{A}})\hat{\mathbf{x}}(s) = \hat{\mathbf{b}}u(s), \\ \hat{y}(s)^2 = \hat{\mathbf{x}}(s)^\mathbf{H}\hat{\mathbf{Q}}\hat{\mathbf{x}}(s), \end{cases} \quad (6)$$

where $\hat{\mathbf{A}}, \hat{\mathbf{E}}, \hat{\mathbf{Q}} \in \mathbb{C}^{r \times r}$, $\hat{\mathbf{b}} \in \mathbb{C}^r$, $\hat{\mathbf{x}}: \mathbb{C} \rightarrow \mathbb{C}^r$ is the approximate internal state and $r \ll n$. In order to be an effective replacement, the approximate system (6) should replicate the input-to-output behaviour of the original large-scale system (5). In other words, given a tolerance $\tau > 0$, the approximate output $\hat{y}: \mathbb{C} \rightarrow \mathbb{C}$ in (6) should satisfy

$$\|y - \hat{y}\| \leq \tau \cdot \|u\|,$$

in appropriate norms and for a range of admissible inputs u .

Considering the classical approach to model systems with the output (2) via linear multi-output systems (3), one advantage is the large variety of established model reduction procedures; see, for example, [2, 6] and the references therein. However, this linearization approach typically necessitates a large number of outputs $p \approx n$. Traditional linear system approximation techniques tend to produce poor quality approximants and require more computational effort when p is large; see [4]. On the other hand, recently there has been a surge of interest in the model reduction of linear quadratic-output systems formulated in the *time domain* [5, 8, 10, 11, 15–17, 19–21]. These systems bear many similarities to the frequency domain linear quadratic-output systems (5) that hold our interest in this work; however, there are subtle differences between these system classes, which we will outline later on.

In this work, we advocate for the treatment of large-scale frequency domain problems, which model the RMS error (2) as quantity of interest using the linear quadratic-output system class (5). A particular example for such a system from the literature is outlined in Section 2. We will make use of some of the established theory for time domain systems, which we review in Section 3, before we discuss classical interpolation approaches for linear systems (3) and propose novel extensions of this interpolation theory for the system class (5) we consider in this work in Section 4. To verify our theoretical results, we apply these new and extended model reduction techniques to the practical example from Section 2 and report the results in Section 5. The paper is concluded in Section 6.

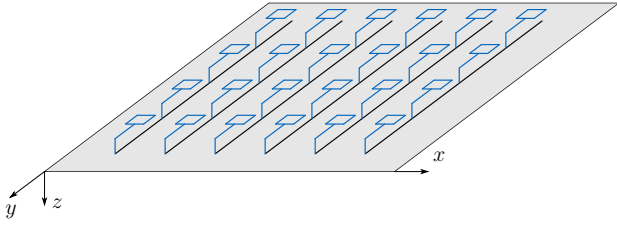


Figure 1: Visual sketch of a plate equipped with TVAs [4].

2 Vibrations of a plate with tuned vibration absorbers

As a specific example for systems of the form (5), we consider the model of the vibrational response of a strutted plate from [4, Sec. 4.2]. The matrices for the computational model itself are available at [3]. The plate has the dimensions 0.8×0.8 m, with a thickness of 1 mm, and it consists of aluminium, with the material parameters $E = 69$ GPa, $\rho = 2650$ kg m $^{-3}$ and $\nu = 0.22$. The damping is assumed to be proportional (Rayleigh damping) with the scaling parameters $\alpha = 0.01$ and $\beta = 1 \cdot 10^{-4}$. The tuned vibration absorbers (TVAs) connected to the plate are used to reduce the vibrational response in the frequency region about 48 Hz. These TVAs are modeled as discrete mass-spring-damper systems.

Acoustical engineers are especially interested in the RMS displacement of the plate points in z -direction in response to point load excitation; cf. Figure 1. This is recovered in [4] using a *second-order* linear-output system of the form

$$\Sigma_{\text{SO,LO}}: \begin{cases} (s^2 \mathbf{M} + s \mathbf{D} + \mathbf{K}) \mathbf{p}(s) = \mathbf{g} u(s), \\ \mathbf{z}(s) = \mathbf{C} \mathbf{p}(s), \end{cases} \quad (7)$$

where $\mathbf{M}, \mathbf{D}, \mathbf{K} \in \mathbb{C}^{n_{\text{so}} \times n_{\text{so}}}$ are the mass, damping, and stiffness matrices, while $\mathbf{g} \in \mathbb{C}^{n_{\text{so}}}$ and $\mathbf{C} \in \mathbb{C}^{p \times n_{\text{so}}}$ are the linear input and output matrices. The internal state $\mathbf{p}: \mathbb{C} \rightarrow \mathbb{C}^{n_{\text{so}}}$ of the plate system contains $n_{\text{so}} = 201\,900$ spatial coordinates that model the position of the plate in the x , y , and z -directions. The RMS displacement of interest is recovered with $p = 27\,278$ entries of the state vector \mathbf{p} , considering only points on the inside of the plate but not on the boundary. This modeling approach is similar to that of (3). For further details on the example, we refer the reader to [4] and the references therein.

Here, instead of the linear outputs in (7), we consider directly the RMS error as the quantity of interest in a *first-order* linear quadratic output system of the form (5). An equivalent system to that of (7) is obtained by rewriting the n_{so} second-order equations in (7) as $n = 2n_{\text{so}}$ *first-order*

equations. Therefore, we define the lifted state

$$\mathbf{x} = \begin{bmatrix} \mathbf{p} \\ s \mathbf{p} \end{bmatrix}: \mathbb{C} \rightarrow \mathbb{C}^n.$$

Then, \mathbf{x} is the state of a system (5) where the system matrices $\mathbf{E}, \mathbf{A}, \mathbf{Q} \in \mathbb{C}^{n \times n}$ and $\mathbf{b} \in \mathbb{C}^n$ are defined in terms of the system matrices in (7) by

$$\begin{aligned} \mathbf{E} &= \begin{bmatrix} \mathbf{I}_{n_{\text{so}}} & \mathbf{0} \\ \mathbf{0} & \mathbf{M} \end{bmatrix}, \quad \mathbf{A} = \begin{bmatrix} \mathbf{0} & \mathbf{I}_{n_{\text{so}}} \\ -\mathbf{K} & -\mathbf{D} \end{bmatrix}, \\ \mathbf{Q} &= \begin{bmatrix} \mathbf{C}^\top \mathbf{C} & \mathbf{0} \\ \mathbf{0} & \mathbf{0} \end{bmatrix}, \quad \mathbf{b} = \begin{bmatrix} \mathbf{0} \\ \mathbf{g} \end{bmatrix}. \end{aligned} \quad (8)$$

The resulting linear quadratic-output system of the form (5) with the system matrices (8) has the dimension $n = 403\,800$. We consider this formulation of the system to construct suitable surrogates of the form (6) that can be used in place of the original large-scale model for the frequency response analysis.

3 Quadratic-output systems in time domain

The description of linear quadratic-output systems in time domain as given in the literature, e.g., [5, 11, 19, 20], strongly resembles the frequency domain formulation (5) that we consider in this work. In the time domain, linear quadratic-output systems are typically represented as

$$\Sigma_{\text{QO}}^t: \begin{cases} \mathbf{E} \dot{\mathbf{x}}_t(t) = \mathbf{A} \mathbf{x}_t(t) + \mathbf{b} u_t(t), & \mathbf{x}_t(0) = \mathbf{0}_n, \\ y_t(t)^2 = \mathbf{x}_t(t)^\top \mathbf{Q} \mathbf{x}_t(t), \end{cases} \quad (9)$$

with $\mathbf{A}, \mathbf{E}, \mathbf{Q} \in \mathbb{R}^{n \times n}$, \mathbf{Q} symmetric, $\mathbf{b} \in \mathbb{R}^n$ and the homogeneous initial condition $\mathbf{x}_t(0) = \mathbf{0}_n$. Similar to (5), the internal state of (9) is denoted as $\mathbf{x}_t: [0, \infty) \rightarrow \mathbb{R}^n$ and the external input as $u_t: [0, \infty) \rightarrow \mathbb{R}$. Despite bearing obvious similarities, the systems (5) and (9) are not equivalent representations connected via the Laplace transformation [9, Chap. 2.6]. In fact, the nonlinear nature of the output equation in (9) prevents the closed representation of the Laplace transform in the frequency domain. An alternative representation for the time domain systems (9) in the Laplace domain is based on the idea of kernel representations and the multivariate Laplace transform; see, e.g., [8]. The resulting multivariate transfer function $H_t: \mathbb{C} \times \mathbb{C} \rightarrow \mathbb{C}$ of (9) is defined as

$$H_t(s_1, s_2) = \mathbf{b}^\top (s_1 \mathbf{E} - \mathbf{A})^{-\top} \mathbf{Q} (s_2 \mathbf{E} - \mathbf{A})^{-1} \mathbf{b}. \quad (10)$$

In contrast, a transfer function of the frequency domain linear quadratic-output system in (5) can be derived as follows: At any point s at which the matrix pencil $s \mathbf{E} - \mathbf{A}$

is nonsingular, the state $\mathbf{x}(s)$ of the system in (5) is given explicitly by

$$\mathbf{x}(s) = (s\mathbf{E} - \mathbf{A})^{-1}\mathbf{b}u(s).$$

Inserting $\mathbf{x}(s)$ into the output equation of (5) reveals the input-to-output relationship of the system to be given as

$$\begin{aligned} y(s) &= ((s\mathbf{E} - \mathbf{A})^{-1}\mathbf{b}u(s))^H \mathbf{Q}(s\mathbf{E} - \mathbf{A})^{-1}\mathbf{b}u(s) \\ &= \mathbf{b}^H (s\mathbf{E} - \mathbf{A})^{-H} \mathbf{Q} (s\mathbf{E} - \mathbf{A})^{-1} \mathbf{b} |u(s)|^2. \end{aligned}$$

The scalar-valued function $H: \mathbb{C} \rightarrow \mathbb{C}$, defined as

$$H(s) = \mathbf{b}^H (s\mathbf{E} - \mathbf{A})^{-H} \mathbf{Q} (s\mathbf{E} - \mathbf{A})^{-1} \mathbf{b}, \quad (11)$$

is the transfer function of the frequency domain linear quadratic-output system (5). Compared to H_t in (10), there are some notable differences. The transfer function (11) is univariate, and has a physical interpretation in terms of the input-to-output mapping of (5) via $y(s) = H(s)|u(s)|^2$. Additionally, this transfer function (11) depends explicitly on the complex conjugate of its argument, \bar{s} , and is thus *not analytic* on its domain, whereas the transfer function (10) is analytic in both independent arguments.

The construction of reduced-order models for linear quadratic-output systems has received increased consideration in recent years. Proposed model reduction methods can broadly be categorized as approaches that are based on energy functionals and balancing of the corresponding system states [5, 15, 16, 20], and the rational interpolation of transfer functions in the frequency domain [8, 10, 11, 17, 19, 21]. Except for [20, 21], all of these works consider solely time domain quadratic-output systems (9) and their corresponding multivariate transfer functions (10). The works [20, 21] do consider in parts also the frequency domain system (5) but only via the intermediate representation using a fully linear system of the form (3), which as outlined above has several disadvantages.

Since we consider in this work the linear quadratic-output system (5) in the frequency domain with the explicit transfer function (11), we primarily focus on interpolatory methods that aim for an accurate approximation of this transfer function. To this end, we will make use of the theory and ideas developed in [8, 10, 17] for time domain linear quadratic-output systems as well as propose a new interpolatory framework for the system class (5) that we consider in this work.

4 Interpolation of linear quadratic-output systems

In the following, we present interpolation-based model order reduction for frequency domain linear quadratic-output systems (5). First, we give an overview about projection-based

model reduction and interpolatory methods for the linear system case (3). Afterwards, we present new results that show how to enforce Lagrange and Hermite interpolation conditions for (11) via projection of the system matrices.

4.1 Projection-based model order reduction

Consider the linear quadratic-output system (5) and some given reduction order $r \ll n$. In projection-based model order reduction, right and left basis matrices $\mathbf{V} \in \mathbb{C}^{n \times r}$ and $\mathbf{W} \in \mathbb{C}^{n \times r}$ corresponding to r -dimensional projection spaces $\text{span}(\mathbf{V})$ and $\text{span}(\mathbf{W})$ are chosen so that the reduced-order model (6) is constructed as

$$\begin{aligned} \hat{\mathbf{E}} &= \mathbf{W}^H \mathbf{E} \mathbf{V}, & \hat{\mathbf{A}} &= \mathbf{W}^H \mathbf{A} \mathbf{V}, \\ \hat{\mathbf{b}} &= \mathbf{W}^H \mathbf{b}, & \hat{\mathbf{Q}} &= \mathbf{V}^H \mathbf{Q} \mathbf{V}. \end{aligned} \quad (12)$$

The corresponding transfer function of the resulting reduced-order model (6) is given by

$$\hat{H}(s) = \hat{\mathbf{b}}^H (s\hat{\mathbf{E}} - \hat{\mathbf{A}})^{-H} \hat{\mathbf{Q}} (s\hat{\mathbf{E}} - \hat{\mathbf{A}})^{-1} \hat{\mathbf{b}}. \quad (13)$$

Note that the same projection framework can be analogously applied to compute reduced-order models of the time domain system (9). In this case, the transfer function of the reduced-order time domain system is given by

$$\hat{H}_t(s_1, s_2) = \hat{\mathbf{b}}^T (s_1 \hat{\mathbf{E}} - \hat{\mathbf{A}})^{-T} \hat{\mathbf{Q}} (s_2 \hat{\mathbf{E}} - \hat{\mathbf{A}})^{-1} \hat{\mathbf{b}}. \quad (14)$$

In the purely linear setting (3), the concept of projection-based model order reduction is essentially the same. The only difference is that in the output equation $\hat{\mathbf{C}} = \mathbf{C} \mathbf{V}$ replaces $\hat{\mathbf{Q}}$ in (12) such that the resulting reduced-order transfer function of the linear-output model becomes

$$\hat{\mathbf{G}}(s) = \hat{\mathbf{C}} (s\hat{\mathbf{E}} - \hat{\mathbf{A}})^{-1} \hat{\mathbf{b}}. \quad (15)$$

It is important to note that the reduced-order system is determined only by the choice of the projection spaces $\text{span}(\mathbf{V})$ and $\text{span}(\mathbf{W})$ rather than the specific realization of the basis matrices \mathbf{V} and \mathbf{W} ; cf., [2, Sec. 3.3]. A classical choice to avoid ill-conditioned computations with the reduced-order model is to replace any primitive constructions of \mathbf{V} and \mathbf{W} with orthogonal matrices computed via, for example, a QR factorization or SVD. In the special case that \mathbf{A} and \mathbf{E} are Hermitian or only one of the two projection spaces can be computed, one typically sets $\mathbf{W} = \mathbf{V}$. This setting is known in the literature as *Galerkin projection*, while the general case with $\mathbf{W} \neq \mathbf{V}$ and $\text{span}(\mathbf{V}) \neq \text{span}(\mathbf{W})$ is referred to as *Petrov-Galerkin projection*. In essence, any projection-based model order reduction method amounts to choosing \mathbf{V} and \mathbf{W} . In the following sections, we consider the construction of the basis matrices such that interpolation of the transfer function is enforced at selected points in the complex plane.

4.2 Interpolatory model reduction for linear systems

In this section, we consider the interpolation-based model reduction of the linear-output systems of the form (3). Interpolation-based model reduction of linear systems is a well-studied subject in the literature. The theoretical foundation for projection-based interpolation has been laid in [7], which was later developed into a numerically efficient framework based on rational Krylov subspaces [12].

Consider a linear system of the form (3) and given complex interpolation points $\sigma_1, \dots, \sigma_k \in \mathbb{C}$. The idea of interpolatory methods is to construct a reduced-order linear model with the corresponding transfer function $\hat{\mathbf{G}}$ of the form (15) so that $\hat{\mathbf{G}}$ interpolates the full-order transfer function \mathbf{G} in (4) at the selected points, i.e.

$$\mathbf{G}(\sigma_i) = \hat{\mathbf{G}}(\sigma_i), \quad (16)$$

for all $i = 1, \dots, k$. In the case of Hermite interpolation, additional conditions are set for the derivatives of the transfer functions to satisfy

$$\frac{d^{j_i}}{ds^{j_i}} \mathbf{G}(\sigma_i) = \frac{d^{j_i}}{ds^{j_i}} \hat{\mathbf{G}}(\sigma_i), \quad (17)$$

for $i = 1, \dots, k$ and some $1 \leq j_i \leq j$. Because the full and reduced-order transfer functions \mathbf{G} and $\hat{\mathbf{G}}$ assume values in \mathbb{C}^p , enforcing interpolation of the entire transfer function can quickly lead to reduced models of high orders when p is large. Recall that this is typically the case when rewriting the RMS error measure (2) into linear-output form. A popular approach to remedy this is imposing interpolation conditions into tangential directions: Given the interpolation points $\sigma_1, \dots, \sigma_k \in \mathbb{C}$ as well as the direction vectors $\mathbf{c}_1, \dots, \mathbf{c}_k \in \mathbb{C}^p$, the tangential interpolation conditions associated with (16) are

$$\mathbf{c}_i^H \mathbf{G}(\sigma_i) = \mathbf{c}_i^H \hat{\mathbf{G}}(\sigma_i),$$

for $i = 1, \dots, k$. Hermite tangential interpolation conditions analogous to (17) can be enforced as well; see [2, Thm. 3.3.2] for more details.

The construction of appropriate interpolants can be done via projection. Assume that the basis matrices $\mathbf{V} \in \mathbb{C}^{n \times r}$ and $\mathbf{W} \in \mathbb{C}^{n \times r}$ are chosen so that

$$\begin{aligned} (\sigma_i \mathbf{E} - \mathbf{A})^{-1} \mathbf{b} &\in \text{span}(\mathbf{V}) \quad \text{and} \\ (\sigma_i \mathbf{E} - \mathbf{A})^{-H} \mathbf{C}^H \mathbf{c} &\in \text{span}(\mathbf{W}) \end{aligned}$$

hold, for $i = 1, \dots, k$, then the reduced-order transfer function $\hat{\mathbf{G}}$ that is constructed via projection will be a tangential Hermite interpolant of the full-order transfer function

\mathbf{G} at the designated points and along the tangential directions [2, Thm. 3.3.1].

The choice of interpolation points is a crucial element in interpolatory model-order reduction, which ultimately determines the performance of the reduced-order model. To select good or even optimal interpolation points, different approximation error measures have been used in the literature. The most common one is the \mathcal{H}_2 -norm, for which locally optimal reduced-order models can be constructed via tangential Hermite interpolation [13, 14]. The associated interpolation points are the mirror images of the eigenvalues of the reduced-order matrix pencil $\lambda \hat{\mathbf{E}} - \hat{\mathbf{A}}$ and the tangential directions are the corresponding transfer function residues. The iterative rational Krylov algorithm (IRKA) is an efficient approach to compute these optimal interpolation points and tangential directions via iterative updates [13]. A different error measure is the \mathcal{L}_∞ -norm, for which typically greedy procedures are used that select interpolation points iteratively as maxima of the error transfer function $\mathbf{G} - \hat{\mathbf{G}}$; see, for example, [1, 4].

4.3 Interpolation in the quadratic-output setting

The aforementioned interpolation of linear systems can be extended to the time domain quadratic-output systems (9). For the transfer function (10), given a set of interpolation points $\sigma_1, \dots, \sigma_k \in \mathbb{C}$, the multivariate interpolation problem is to find \hat{H}_t such that

$$H_t(\sigma_i, \sigma_j) = \hat{H}_t(\sigma_i, \sigma_j)$$

holds, for $i, j = 1, \dots, k$. As in the linear setting, these interpolation conditions can be enforced via projection using rational Krylov subspaces; see [8, Cor. 1]. The work [17] shows that \mathcal{H}_2 -optimal interpolants for time domain systems of the form (9) satisfy the following Hermite interpolation conditions

$$H_t(-\bar{\lambda}_i, -\bar{\lambda}_j) = \hat{H}_t(-\bar{\lambda}_i, -\bar{\lambda}_j),$$

and

$$\begin{aligned} &\sum_{k=1}^r \left(\hat{q}_{i,k} \frac{\partial}{\partial s_1} H_t(-\bar{\lambda}_i, -\bar{\lambda}_k) + \hat{q}_{k,i} \frac{\partial}{\partial s_2} H_t(-\bar{\lambda}_k, -\bar{\lambda}_i) \right) \\ &= \sum_{k=1}^r \left(\hat{q}_{i,k} \frac{\partial}{\partial s_1} \hat{H}_t(-\bar{\lambda}_i, -\bar{\lambda}_k) + \hat{q}_{k,i} \frac{\partial}{\partial s_2} \hat{H}_t(-\bar{\lambda}_k, -\bar{\lambda}_i) \right), \end{aligned}$$

for $i, j = 1, \dots, r$, where $\lambda_1, \dots, \lambda_r \in \mathbb{C}$ are the eigenvalues of the reduced-order matrix pencil $\lambda \hat{\mathbf{E}} - \hat{\mathbf{A}}$ in (12), and $\hat{q}_{i,j} \in \mathbb{C}$ denotes the (i, j) -th entry of $\hat{\mathbf{Q}} \in \mathbb{C}^{r \times r}$ in an appropriate basis. Based on these interpolation conditions,

a generalization of the IRKA approach for systems of the form (9) is proposed in [17]. Due to the similarities between (5) and (9) as well as their transfer functions (10) and (11), we expect this IRKA-like approach to be well suited for constructing accurate projection spaces for the frequency domain quadratic-output system (5), too.

In the following, we develop a new projection-based interpolation theory for the frequency domain quadratic-output system (5). As previously mentioned, the transfer function (11) is not analytic such that Hermite interpolation requires special care. However, in most instances, the interpolation points for model order reduction are selected only from the imaginary axis [1, 4]. Considering $z \in i\mathbb{R}$, the transfer function (11) simplifies to

$$H(z) = \mathbf{b}^H(-z\mathbf{E}^H - \mathbf{A}^H)^{-1}\mathbf{Q}(z\mathbf{E} - \mathbf{A})^{-1}\mathbf{b}. \quad (18)$$

In this case, the transfer function (18) is differentiable along the imaginary axis, which leads to the following theorem.

Theorem 1. *Let $H: i\mathbb{R} \rightarrow \mathbb{C}$ be the transfer function (11) and $\hat{H}: i\mathbb{R} \rightarrow \mathbb{C}$ be the reduced-order transfer function (13) obtained via projection (6), both restricted to the imaginary axis. Consider interpolation points $z_1, \dots, z_k \in i\mathbb{R}$, in which H and \hat{H} can be evaluated, and the basis matrices $\mathbf{V} \in \mathbb{C}^{n \times r}$ and $\mathbf{W} \in \mathbb{C}^{n \times r}$ satisfy*

$$(z_i\mathbf{E} - \mathbf{A})^{-1}\mathbf{b} \in \text{span}(\mathbf{V}), \quad (19)$$

$$(z_i\mathbf{E} - \mathbf{A})^{-H}\mathbf{Q}(z_i\mathbf{E} - \mathbf{A})^{-1}\mathbf{b} \in \text{span}(\mathbf{W}), \quad (20)$$

for $i = 1, \dots, k$. Then, for $i = 1, \dots, k$, the following interpolation conditions hold:

$$H(z_i) = \hat{H}(z_i) \quad \text{and} \quad \frac{d}{dz}H(z_i) = \frac{d}{dz}\hat{H}(z_i).$$

Proof. Set $\mathcal{K}(z) = z\mathbf{E} - \mathbf{A}$, $\hat{\mathcal{K}}(s) = s\hat{\mathbf{E}} - \hat{\mathbf{A}}$, $\mathbf{v}_i = \hat{\mathcal{K}}(z_i)^{-1}\hat{\mathbf{b}}$ and $\mathbf{w}_i = \hat{\mathcal{K}}(z_i)^{-H}\hat{\mathbf{Q}}\hat{\mathcal{K}}(z_i)^{-1}\hat{\mathbf{b}}$. By construction of \mathbf{V} and \mathbf{W} , the following two projection identities hold

$$\mathbf{V}\mathbf{v}_i = \mathcal{K}(z_i)^{-1}\mathbf{b}, \quad \mathbf{W}\mathbf{w}_i = \mathcal{K}(z_i)^{-H}\mathbf{Q}\mathcal{K}(z_i)^{-1}\mathbf{b};$$

see, e.g., [22] for details on the projectors. It follows that

$$\hat{H}(z_i) = \mathbf{v}_i^H \hat{\mathbf{Q}} \mathbf{v}_i = \mathbf{v}_i^H \mathbf{V}^H \mathbf{Q} \mathbf{V} \mathbf{v}_i = H(z_i)$$

holds, for $i = 1, \dots, k$. The derivative of the reduced-order transfer function is given via

$$\frac{d}{dz}\hat{H}(z_i) = \mathbf{v}_i^H \hat{\mathbf{E}}^H \mathbf{w}_i - \mathbf{w}_i^H \hat{\mathbf{E}} \mathbf{v}_i.$$

Applying both the identities above yields

$$\frac{d}{dz}\hat{H}(z_i) = \mathbf{v}_i^H \mathbf{V}^H \mathbf{E}^H \mathbf{W} \mathbf{w}_i - \mathbf{w}_i^H \mathbf{W}^H \mathbf{E} \mathbf{V} \mathbf{v}_i = \frac{d}{dz}H(z_i),$$

for $i = 1, \dots, k$, which concludes the proof. \square

The Lagrange interpolation condition in Theorem 1 is similar to the result in [8, Cor. 1] for multivariate transfer functions (10). However, Theorem 1 is specifically tailored for (11), which we consider in this paper, and provides new Hermite interpolation results. Note that due to the structure of the primitive bases vectors in (19) and (20), the basis matrices $\mathbf{V} \in \mathbb{C}^{n \times r}$ and $\mathbf{W} \in \mathbb{C}^{n \times r}$ can be computed efficiently by solving linear systems of equations. If the Hermite interpolation conditions are not required, \mathbf{W} can also be used to match additional Lagrange interpolation conditions by mimicking the structure of \mathbf{V} at additional points.

5 Numerical experiments

In the following, we apply the interpolatory model-order reduction schemes from Section 4 to the vibrating plate model in Section 2. The experiments reported here have been executed on the Gauss compute server of the Department of Mathematics at Virginia Tech. This machine is equipped with 4 Intel(R) Xeon(R) CPU E7-4890 v2 processors running at 3.17 GHz and 1 TB total main memory. It is running on Ubuntu 22.04.3 LTS and uses MATLAB 23.2.0.2365128 (R2023b). The source code for the numerical experiments and the computed results are available at [18].

5.1 Experimental setup

For the model reduction of frequency domain quadratic-output systems (5), we propose and compare five different interpolation-based approaches as described in the following:

LQO-IRKA is the time domain quadratic-output IRKA that we apply to the matrices of the frequency domain system as described in Section 4;

Int_{∞,V} performs interpolation following Theorem 1 using a Galerkin projection based on (19) and selecting interpolation points greedily from a pre-sampled basis;

Int_{∞,VW} is the same as Int_{∞,V} but with a Petrov-Galerkin projection using (19) and (20);

Int_{avg,V} uses a Galerkin projection based on a truncated approximation of a pre-sampled interpolation basis as in Theorem 1 and (19) computed by the pivoted QR decomposition,

Int_{avg,VW} is the same as Int_{avg,V} but with a Petrov-Galerkin projection using two pre-sampled bases following (19) and (20).

The latter four of these methods (Int_{*}) rely on a pre-sampled basis, for which we compute and save the solutions to (19)

and (20) in 250 linearly equidistant points in the interval $i[1, 2\pi \cdot 251] \subset i\mathbb{R}$.

To visibly compare different approximations, we use the pointwise relative approximation errors of the transfer functions as

$$\text{relerr}(\omega) = \frac{|H(2\pi i \cdot \omega) - \hat{H}(2\pi i \cdot \omega)|}{|H(2\pi i \cdot \omega)|}, \quad (21)$$

for the frequencies $\omega \in [0, 250]$ Hz, in plots alongside the magnitude of the transfer functions. Additionally, we score the performance of the proposed methods based on two relative system error measures. To compare the average performance of the computed reduced models over the frequency range $i[0, 2\pi \cdot 250] \subset i\mathbb{R}$, we compute an approximation to the relative \mathcal{H}_2 error as

$$\text{relerr}_{\mathcal{H}_2} = \frac{\sum_{i=0}^{500} |H(2\pi i \cdot \omega_i) - \hat{H}(2\pi i \cdot \omega_i)|}{\sum_{i=0}^{500} |H(2\pi i \cdot \omega_i)|}, \quad (22)$$

where $\Omega = \{\omega_i\}_{i=1}^{500}$ is the collection of 500 linearly equidistant points in the interval $[0, 250] \subset \mathbb{R}$. Also, to compare the worst case performance of the computed reduced models over the frequency range $[0, 250]$ Hz, we compute the following approximation to the relative \mathcal{H}_∞ error via

$$\text{relerr}_{\mathcal{H}_\infty} = \frac{\max_{\omega_i \in \Omega} |H(2\pi i \cdot \omega_i) - \hat{H}(2\pi i \cdot \omega_i)|}{\max_{\omega_i \in \Omega} |H(2\pi i \cdot \omega_i)|}, \quad (23)$$

where Ω is the set of 500 frequency points as defined above.

5.2 Discussion

We computed reduced-order models of orders $r = 25, 50, 75$ and 100 using the five approaches described in the previous section. The performance of the computed reduced models for orders $r = 50$ and $r = 75$ in the considered frequency range is shown Figure 2 in terms of the transfer function magnitudes and the pointwise relative approximation errors (21). The relative approximate system norm errors for each method and all four reduction orders r are recorded in Tables 1 and 2.

We observe that all compared methods provide reasonably accurate approximations for all considered orders of reduction $r = 25, 50, 75, 100$. For the $r = 50$ reduced-order model in Figure 2, it is evident that the errors of $\text{Int}_{\infty, V}$ and $\text{Int}_{\infty, VW}$ are multiple orders of magnitude smaller for lower frequencies compared to the other three methods. Similar behavior could be observed for the $r = 25$ reduced model; see the accompanying code package for these results [18] as well as for $r = 100$. This comes from the use of the absolute \mathcal{H}_∞ error measure in the greedy approaches. On the

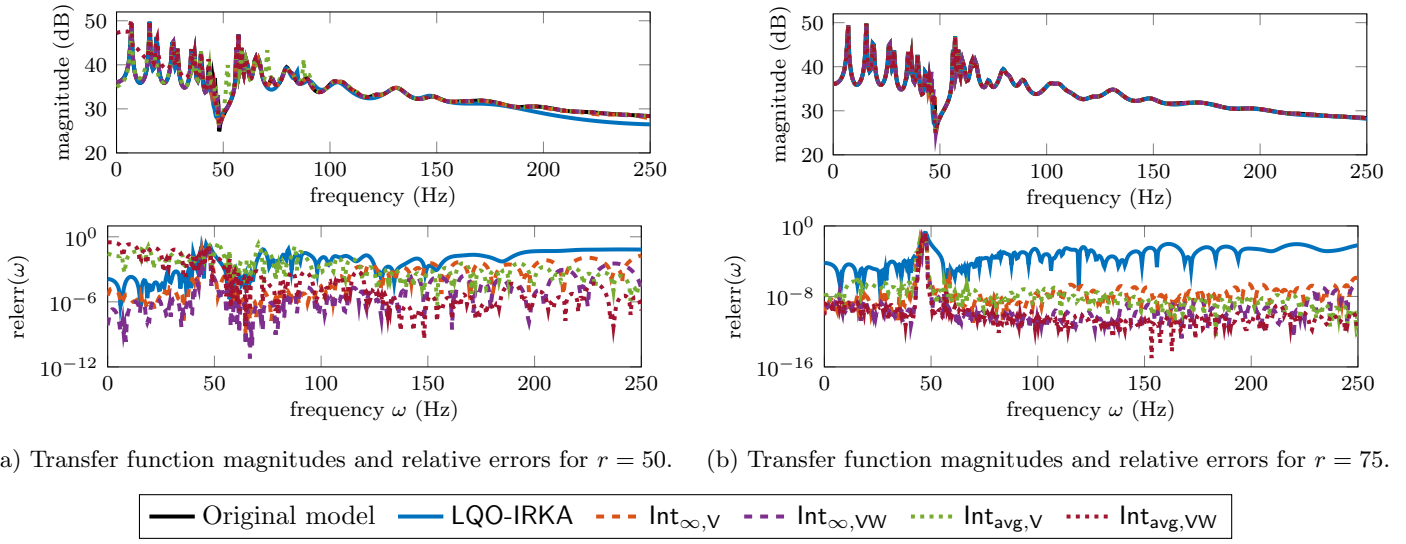
Table 1: Relative \mathcal{H}_2 errors according to (22) for reduced-order models of size $r = 25, 50, 75, 100$. The smallest error for each order is highlighted in **boldface**.

	$r = 25$	$r = 50$	$r = 75$	$r = 100$
LQO-IRKA	1.071e-1	1.973e-2	2.529e-3	1.017e-3
$\text{Int}_{\infty, V}$	1.119e-1	2.466e-3	7.357e-4	9.801e-4
$\text{Int}_{\infty, VW}$	7.013e-2	1.005e-3	4.616e-4	3.841e-4
$\text{Int}_{\text{avg}, V}$	1.020e-1	1.145e-2	5.722e-4	5.015e-4
$\text{Int}_{\text{avg}, VW}$	2.364e-1	1.783e-1	4.674e-4	5.519e-4

Table 2: Relative \mathcal{H}_∞ errors according to (23) for reduced-order models of size $r = 25, 50, 75, 100$. The smallest error for each order is highlighted in **boldface**.

	$r = 25$	$r = 50$	$r = 75$	$r = 100$
LQO-IRKA	2.169e-1	1.539e-1	1.066e-1	6.436e-2
$\text{Int}_{\infty, V}$	1.769e-1	8.872e-2	9.475e-2	1.168e-1
$\text{Int}_{\infty, VW}$	1.569e-1	9.291e-2	5.030e-2	6.076e-2
$\text{Int}_{\text{avg}, V}$	5.159e-1	1.918e-1	6.368e-2	9.623e-2
$\text{Int}_{\text{avg}, VW}$	7.023e-1	2.254e-1	1.058e-1	8.828e-2

other hand, $\text{Int}_{\text{avg}, V}$ and $\text{Int}_{\text{avg}, VW}$ provide a better approximation for higher frequencies through the basis approximation since all frequencies are considered to be about equally important here. This leads to less accurate approximations for lower frequencies, where a lot of the dominant transfer function behavior happens. LQO-IRKA exhibits an overall similar approximation behavior. Note that $\text{Int}_{\infty, VW}$ and $\text{Int}_{\text{avg}, VW}$, which include information about the nonlinear output equation, perform visibly better than their Galerkin counterparts that only account for the linear input-to-state equation. This can also be seen in Tables 1 and 2. The relative error values of $\text{Int}_{\infty, VW}$ and $\text{Int}_{\text{avg}, VW}$ are smaller than their Galerkin counterparts for almost every order of reduction. For $r = 75$ and $r = 100$, the LQO-IRKA iteration did not converge in the prescribed number of steps such that its approximation accuracy cannot keep up with the other approaches, which appear to have reached the smallest possible error for most of the frequency interval. We note that for any order, the frequency 48 Hz is difficult to match due to the use of the TVAs; see [4]. This could be resolved by additionally enforcing interpolation at this particular point. Lastly, for every order of reduction and in each metric, the greedy sampling-based methods $\text{Int}_{\infty, V}$ and $\text{Int}_{\infty, VW}$ exhibit the smallest magnitude errors, with $\text{Int}_{\infty, VW}$ performing better in almost every instance. This holds true even in the relative \mathcal{H}_2 error metric (22), despite the expectation that the averaging-based approaches may



(a) Transfer function magnitudes and relative errors for $r = 50$. (b) Transfer function magnitudes and relative errors for $r = 75$.

Figure 2: Frequency response results for reduced-order models of orders $r = 50$ and $r = 75$: All proposed methods provide reasonably accurate approximations of the original system behavior. The interpolation methods that take the output equation into account provide visibly more accurate results than the classical Galerkin-based methods. LQO-IRKA performs multiple orders of magnitude worse for $r = 75$ compared to the other methods due to the method not converging in the prescribed amount of iteration steps.

perform better here.

6 Conclusions

In this work, we presented model order reduction approaches for systems with root mean squared error measures in the frequency domain. We provided a new theoretical framework for Hermite interpolation of such systems and showed in numerical experiments that interpolation methods based on this new theory outperform classical approaches that rely on the linearization of the measured quantities. The LQO-IRKA method transcribed from time domain quadratic-output systems performed comparably well when it converged, which leads to the question if one can design a similar optimization procedure for the frequency domain systems that we considered in this work.

Acknowledgments

The authors would like to thank Serkan Gugercin for inspiring discussions.

References

- [1] N. Aliyev, P. Benner, E. Mengi, and M. Voigt. A subspace framework for \mathcal{H}_∞ -norm minimization. *SIAM J. Matrix Anal. Appl.*, 41(2):928–956, 2020. doi:10.1137/19M125892X.
- [2] A. C. Antoulas, C. A. Beattie, and S. Gugercin. *Interpolatory Methods for Model Reduction*. Computational Science & Engineering. SIAM, Philadelphia, PA, 2020. doi:10.1137/1.9781611976083.
- [3] Q. Aumann and S. W. R. Werner. Code, data and results for numerical experiments in “Structured model order reduction for vibro-acoustic problems using interpolation and balancing methods” (version 1.1), August 2022. doi:10.5281/zenodo.6806016.
- [4] Q. Aumann and S. W. R. Werner. Structured model order reduction for vibro-acoustic problems using interpolation and balancing methods. *J. Sound Vib.*, 543:117363, 2023. doi:10.1016/j.jsv.2022.117363.
- [5] P. Benner, P. Goyal, and I. Pontes Duff. Gramians, energy functionals, and balanced truncation for linear dynamical systems with quadratic outputs. *IEEE Trans. Autom. Control*, 67(2):886–893, 2021. doi:10.1109/TAC.2021.3086319.

- [6] P. Benner, V. Mehrmann, and D. C. Sorensen. *Dimension Reduction of Large-Scale Systems*, volume 45 of *Lect. Notes Comput. Sci. Eng.* Springer, Berlin, Heidelberg, 2005. doi:10.1007/3-540-27909-1.
- [7] C. De Villemagne and R. E. Skelton. Model reductions using a projection formulation. *Int. J. Control*, 46(6):2141–2169, 1987. doi:10.1080/00207178708934040.
- [8] A. N. Diaz, M. Heinkenschloss, I. V. Gosea, and A. C. Antoulas. Interpolatory model reduction of quadratic-bilinear dynamical systems with quadratic-bilinear outputs. *Adv. Comput. Math.*, 49(6):95, 2023. doi:10.1007/s10444-023-10096-2.
- [9] G. E. Dullerud and F. Paganini. *A Course in Robust Control Theory: A Convex Approach*, volume 36 of *Texts in Applied Mathematics*. Springer, New York, NY, 2000. doi:10.1007/978-1-4757-3290-0.
- [10] I. V. Gosea and A. C. Antoulas. A two-sided iterative framework for model reduction of linear systems with quadratic output. In *2019 IEEE 58th Conference on Decision and Control (CDC)*, pages 7812–7817, 2019. doi:10.1109/CDC40024.2019.9030025.
- [11] I. V. Gosea and S. Gugercin. Data-driven modeling of linear dynamical systems with quadratic output in the AAA framework. *J. Sci. Comput.*, 91(1):16, 2022. doi:10.1007/s10915-022-01771-5.
- [12] E. J. Grimme. *Krylov projection methods for model reduction*. PhD thesis, University of Illinois, Urbana-Champaign, USA, 1997. URL: <https://perso.uclouvain.be/paul.vandooren/ThesisGrimme.pdf>.
- [13] S. Gugercin, A. C. Antoulas, and C. Beattie. \mathcal{H}_2 model reduction for large-scale linear dynamical systems. *SIAM J. Matrix Anal. Appl.*, 30(2):609–638, 2008. doi:10.1137/060666123.
- [14] L. Meier and D. Luenberger. Approximation of linear constant systems. *IEEE Trans. Autom. Control*, 12(5):585–588, 1967. doi:10.1109/TAC.1967.1098680.
- [15] R. Pulch. Energy-based model order reduction for linear stochastic Galerkin systems of second order. *Proc. Appl. Math. Mech.*, 23(3):e202300038, 2023. doi:10.1002/pamm.202300038.
- [16] R. Pulch and A. Narayan. Balanced truncation for model order reduction of linear dynamical systems with quadratic outputs. *SIAM J. Sci. Comput.*, 41(4):A2270–A2295, 2019. doi:10.1137/17M1148797.
- [17] S. Reiter, I. Pontes Duff, I. V. Gosea, and S. Gugercin. \mathcal{H}_2 -optimal model reduction of linear systems with quadratic outputs. Nonlinear Model Reduction for Control, Virginia Tech, 2023. doi:10.5281/zenodo.10712995.
- [18] S. Reiter and S. W. R. Werner. Code and results for numerical experiments in “Interpolatory model order reduction of large-scale dynamical systems with root mean squared error measures” (version 1.1), June 2024. doi:10.5281/zenodo.11557038.
- [19] Sean Reiter, Igor Pontes Duff, Ion Victor Gosea, and Serkan Gugercin. \mathcal{H}_2 optimal model reduction of linear systems with multiple quadratic outputs. e-prints 2405.05951, arXiv, 2024. URL: <https://arxiv.org/abs/2405.05951>.
- [20] R. Van Beeumen and K. Meerbergen. Model reduction by balanced truncation of linear systems with a quadratic output. *AIP Conf. Proc.*, 1281:2033–2036, 2010. doi:10.1063/1.3498345.
- [21] R. Van Beeumen, K. Van Nimmen, G. Lombaert, and K. Meerbergen. Model reduction for dynamical systems with quadratic output. *Int. J. Numer. Methods Eng.*, 91(3):229–248, 2012. doi:10.1002/nme.4255.
- [22] S. W. R. Werner. *Structure-Preserving Model Reduction for Mechanical Systems*. Dissertation, Otto-von-Guericke-Universität, Magdeburg, Germany, 2021. doi:10.25673/38617.